

# Deep tissue microscopic imaging of the kidney with a gradient-index lens system

Xin Li, Weiming Yu\*

*Indiana University School of Medicine, Department of Medicine, Division of Nephrology, 950 W. Walnut Street, R2-268, Indianapolis, IN 46202, United States*

Received 21 June 2007; received in revised form 23 August 2007; accepted 27 August 2007

## Abstract

Intravital microscopy using two-photon excitation is proven to be a valuable tool for studying the kidney and associated disease processes. However, routine performance of intravital kidney imaging is limited by the fact that fluorescence signal is attenuated by the tissue and at certain tissue depth lost its strength completely. For most of the animal tissues, this finite imaging depth is limited to a few hundred microns. Currently it is not possible to non-invasively image the kidney beyond the superficial tissue layers of the cortex. This has imposed significant limitations on the animal models one can use for imaging since structure such the glomerulus is typically located below the superficial layer of the cortex that cannot be imaged using a conventional fluorescence microscope. Here we report the use of a needle-like lens system based on gradient-index (GRIN) microlenses capable of transferring high quality fluorescence images of the tissue through a regular microscope objective for deep tissue imaging of the kidney. By combining this GRIN lens system with a Zeiss LSM 510 NLO microscope, we are able to extend the depth for imaging kidney tissues far beyond the few hundred microns limit. This GRIN lens imaging system provides an alternative microendoscopic imaging tool that will enhance current intravital kidney imaging techniques for studying structural and functional properties of local tissues at locations below the superficial layers of the kidney.

© 2007 Elsevier B.V. All rights reserved.

*Keywords:* Microendoscopy; Intravital microscopy; Deep tissue imaging; Two-photon excitation; Kidney

## 1. Introduction

Fluorescence microscopy using two-photon excitation has a distinct advantage over one-photon confocal for being able to image deeper into the tissue. This advantage arises primarily from the use of near infrared laser light [1]. Two-photon microscopy has found many *in vivo* applications and becomes one of the most powerful tools for obtaining high resolution intravital images of live specimens, especially when it combined with quantitative data analysis for retrieving dynamic and functional information

[2–4]. The imaging depth in most applications, however, is currently limited to less than 1 mm using conventional microscope objectives. Depending upon the optical properties of the tissues, the imaging depth one can reach using two-photon excitation microscopy can vary significantly. For relatively transparent tissue such as the brain, one can reach as far as 1000  $\mu\text{m}$  below the tissue surface [5]. The useable imaging depth for skin application on the other hand is limited to less than 50  $\mu\text{m}$  [6,7]. In case of intravital applications of the kidney, the imaging depth is limited within about 200  $\mu\text{m}$  [8]. This imaging depth limitation has significantly confined our ability for structural and functional studies of the kidney. For example, in order to visualize and study the glomerulus, the functional unit of the kidney, we are limited to use certain types of animals

\* Corresponding author. Tel.: +1 317 278 4481; fax: +1 317 274 8575.  
E-mail address: [wmyu@iupui.edu](mailto:wmyu@iupui.edu) (W. Yu).

that have superficial glomerulus [9]. On the other, there are many genetically engineered mouse models that do not have superficial glomerulus or other tissue structures of interests that are located immediately below the surface of the cortex. One cannot use these animal models for non-invasive in vivo imaging. However, it is very important to study the kidney below the superficial layers since at the deeper layers where local blood flow, tissue oxygenation level and the cellular metabolism are known to be different from those of the outer layer of the renal cortex. In particular, deep tissue imaging is important for the understanding of the patho-physiology of the tissue regions related to kidney diseases. Here we summarize our work towards extending the imaging depth beyond the 200  $\mu\text{m}$  limit for intravital kidney imaging using a gradient-index (GRIN) lens system combined with a commercial two-photon laser scanning fluorescence microscope.

Gradient-index microlens is a non-conventional lens that typically has a cylindrical shape available in various sizes. The refractive index of the lens varies parabolically along the radius of the lens, having a maximum in the optical axis of the lens (lens center) and gradually decreases towards the outer edge. Fig. 1C depicts the refractive index profile of a GRIN lens as a function of radial position. Due to this refractive index gradient, a light ray strikes on the front surface of the lens follows a sinusoidal path along the lens rod (Fig. 1A). A complete sinusoidal path refers to as a pitch (indicated on Fig. 1A). GRIN lens is convenient for coupling light into fiber optics due to its cylindrical shape and therefore widely used as a component in telecommunication devices. As a lens, it also finds applications in the areas of optical spectroscopy [10,11] and

imaging including optical coherent tomography (OCT) [12,13], endoscopy [14–16] and optical microscopy [17–22]. GRIN lenses were reported to be implemented in conjunction with both confocal and two-photon fluorescence microscopes for in vivo imaging of the brain [18,19,22]. Due to the small size of the GRIN lens (100–1000  $\mu\text{m}$  in diameter), it can be used to facilitate the construction of a miniaturized imaging head for in vivo applications [23] and as a solid immersion lens for deep tissue imaging of live animals [22,24]. In principle, when using the GRIN lens as solid immersion lens, the imaging depth is only limited by how far this needle-like lens can be immersed into the tissue beneath the tissue surface. To date, microscopic or microendoscopic applications using GRIN lens systems were mostly found in imaging of the brain in live rodents [18,19,22]. Recently, an application of using GRIN lens for dermatological inspection of volunteer patients was proposed [21]. We are interested in using a GRIN lens system to extend its microscopic application for intravital deep kidney imaging.

## 2. Laser scanning microendoscopy using GRIN lens probes

For microendoscopic imaging applications, a single GRIN rod lens can be used directly to couple with optical fibers and to achieve axial resolution as high as 3.2  $\mu\text{m}$  [15]. Potential complications of using this simple configuration are associated with the facts that the fluorescence signal level, the axial resolution and the effective numerical aperture (N.A.) of the GRIN lens are varied as functions of the gap distance between the ends of the GRIN lens and the coupling optical fiber [25]. A single high N.A. GRIN rod

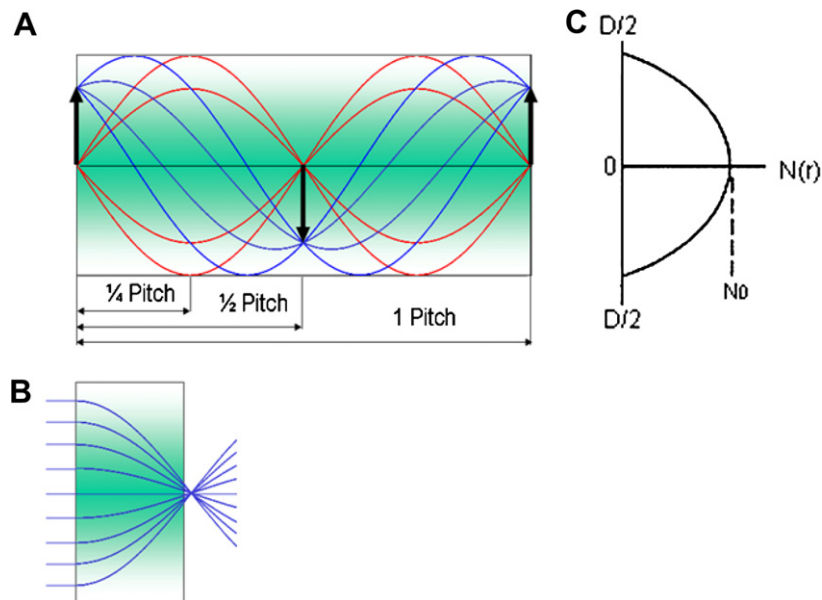


Fig. 1. Gradient-index lenses. (A) GRIN lens with one pitch length and examples of image transfer through a GRIN lens. Images at the entrance surface of a 1/2-pitch lens are inverted at the exit surface. Images transfer through an one pitch long GRIN lens maintain their orientations with a magnification factor of one; (B) GRIN lens with a pitch length slightly shorter than 1/4-pitch; (C) Refractive index profile of a GRIN lens.

lens can also be used directly to couple with a microscope objective with similar or matching numerical aperture for microendoscopic imaging. In this case the pitch length of the GRIN lens to be used can be slightly shorter than the integral multiple of 1/2 pitches [21]. The practical issues of using a single GRIN lens are (1) the physical length of the GRIN lens that can be made useful for deep tissue probing, (2) the diameter of the GRIN lens which is desired to be small for microendoscopic applications and (3) the optical artifacts generated by the GRIN lens (e.g., various nonlinear effects especially when the beam focuses more than once inside the GRIN rod lens) interfering with the signals to be measured. There have been also a number of reports of using compound GRIN lenses in doublet and triplet configurations for in vivo microendoscopy applications [19,22]. A doublet compound GRIN lens probe consists of one objective lens and a relay lens connected directly with each other. Typically the relay lens has a smaller numerical aperture ( $\sim 0.1$ – $0.2$ ) and the end of the relay lens can be coupled to either a focused beam such as in cases of using a low N.A. microscope objective or a simple optical lens for imaging applications [22] or a collimated beam such as in case of using optical fibers [18]. Depending upon the pitch length of the objective GRIN lens one selects to use, the pitch length of the relay lens can be determined accordingly so that images can be transferred properly through the lens system. For example, in a typical case, the length of the objective lens is slightly less than 1/4 of a pitch (Fig. 1B), the relay lens can be an odd integrate multiple of 1/4-pitch when it needs to be coupled with a microscope objective or a simple lens. When a doublet GRIN lens microendoscopic probe with an objective lens slightly shorter than 1/4-pitch coupled directly with a collimated beam [18], the relay lens needs to be an integral multiple of 1/2-pitch. A triplet GRIN lens probe has a coupling lens directly connected to the other end of the relay lens of the above mentioned doublet compound GRIN lens. Triplet GRIN lens probes have been reported in a number of in vivo applications combining with two-photon excitation fluorescence microscopes [19,22]. Similar to the doublet GRIN lens probe, in a typical triplet GRIN lens probe configuration, a GRIN lens with about 1/4 pitches is used as an objective lens, the relay GRIN lens can be any integral multiples of 1/2-pitch and a 1/4-pitch coupling GRIN lens. It is desirable to use a relatively high N.A. coupling lens in the triplet GRIN lens probe to allow it to couple to a regular conventional high N.A. microscope objective. Using a high N.A. objective lens is also desirable for achieving high spatial resolution for imaging applications.

The advantages of using GRIN lenses as microendoscopic probes are: they are versatile and cost effective comparing with using a commercial microscope objective lens made with conventional lenses but having a very small footprint, e.g., the MicroProbe lens (Olympus, Melville, NY). A GRIN lens microendoscopic probe can be designed and assembled relatively easily according to a specific applica-

tion and they can be adapted to work together with regular microscope objectives with different magnifications. Unlike the GRIN lens probes, MicroProbe lenses are less flexible as they are made with fixed and specific magnifications.

### 3. Deep tissue microendoscopy of the kidney

#### 3.1. Microendoscopic imaging system

Of the shelf GRIN lenses were purchased from NSG America, INC (Somerset, NJ) and used directly to assemble the GRIN lens probe. Two 0.6 N.A. imaging lenses (350  $\mu\text{m}$  in diameter and 0.65 mm in length) with 0.22 pitches were glued to each end of a 1 pitch long rod lens (350  $\mu\text{m}$  in diameter and 14.95 mm in length) with 0.1 N.A. using transparent UV curing optical adhesive (Norland Products, Inc., Cranbury, NJ) and protocols similar to what is described by Levene et al. [19]. The two high N.A. imaging lenses are functioning as the objective lens and the coupling lens of the GRIN lens microendoscopic probe, respectively. Thus, the total physical length of the GRIN lens probe was 16.25 mm. The relay rod lens was protected by a metal jacket with an outer diameter of  $\sim 600$   $\mu\text{m}$  to make the microendoscopic probe mechanically durable for deep tissue microendoscopy applications. The assembled GRIN lens probe was hold in place by using a five-axis bare fiber translator (Siskiyou Design Instruments, Grant Pass, OR) which was attached to the body of a Carl Zeiss Plan-Apochromat 20X, 0.75 N.A. air immersion objective of an Axioplan 2 (upright) microscope (as illustrated in Fig. 2). This microscope is part of the LSM 510 Meta NLO microscope system (Carl Zeiss, Inc., Thornwood, NY) we use, and it is equipped with a Tsunami Ti-sapphire laser (Spectra-Physics, Mountain View, CA) pumped by a 10 Watt Millennia Xs all-solid-state laser (Spectra-Physics, Mountain View, CA). Therefore, the relative position between the microscope objective and the compound GRIN lens probe was fixed while the Z-control motor of the Axioplan microscope that controls the Z position of the microscope stage can be adjusted for microendoscopic imaging applications. The coupling and alignment of the compound GRIN lens microendoscopic probe with the microscope objective can be accomplished by adjusting the axis controls of the fiber translator. The fairness of the alignment was judged by imaging a piece of Kodak lens cleaning paper in obtaining the fluorescence signal and the resolution of the fluorescence image. For imaging experiments, the Ti-sapphire laser was tuned to 800 nm with less than 50 mW of power at the sample for two-photon excitation in both cases of the in vitro and the in vivo applications. The transmission efficiency of the compound GRIN lens probe depends on how well the three pieces of GRIN lenses glued together and it can reach as high as 70% to 800 nm laser light. The coupling efficiency between the 20X, 0.75 N.A. Plan-Apochromat objective and the compound GRIN lens probe was  $\sim 58\%$ . This yielded an overall laser scanning excitation

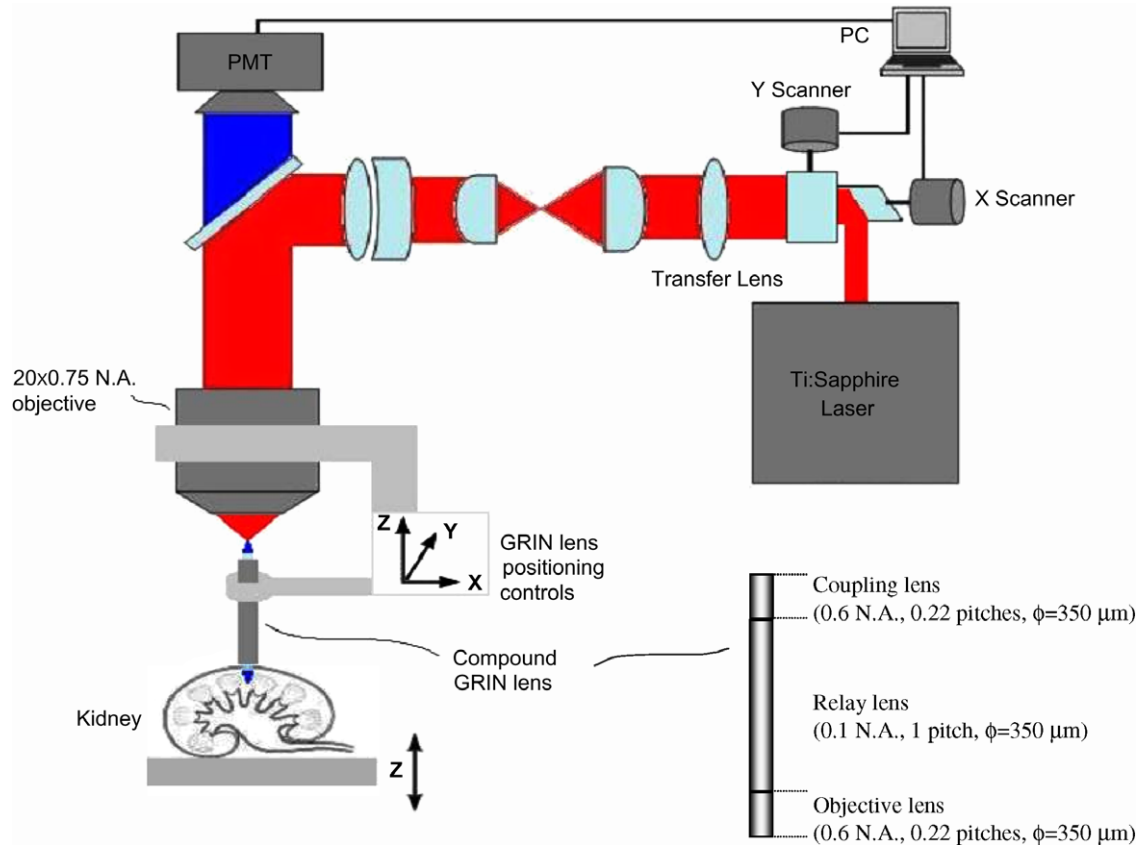


Fig. 2. Schematics of the imaging system. GRIN lens probe is used in conjunction with a Carl Zeiss LSM 510 two-photon microscope. The triplet GRIN lens microendoscopic probe is attached to a 20X air objective through a 5-axis optical fiber translator. The Z-control motor moves the sample stage which carries the kidney tissue samples or live animals for microendoscopic imaging.

throughput slightly better than 40% similar to what's reported in the literature [19] in a similar configuration.

### 3.2. Sample preparation

Lipid membrane probe Prodan and cell nuclear dye Hoechst 33342 were purchased from Invitrogen (Eugene, OR). Prodan stock solution was made by dissolving the fluorophore in DMSO to a final concentration of 2 mM. For in vitro microendoscopic imaging experiments, a freshly excised kidney from a male Sprague-Dawley rat was perfused with 0.9% Phosphate Buffered Saline (PBS) containing a Prodan concentration of 20  $\mu\text{M}$  and the dye solution was left in the kidney for 2 h before washing it out with a 0.9% PBS solution. For in vivo imaging experiments, 6–8 week old male healthy Sprague-Dawley rats, about 200 g in weight, were prepared using the procedures described before [9]. Cell nuclear dye was intravenously infused  $\sim 30$  min before imaging acquisition. One kidney of the rat was externalized and hold in a custom-made micropuncture kidney cup for imaging experiment [26]. Before performing microendoscopic imaging for both the in vivo and ex vivo samples, a small puncture through the capsule of the kidney and into the cortex was performed with a 28 gauge needle for facilitating the insertion of the GRIN lens probe.

### 3.3. Image data analysis

Microendoscopic images of the kidney were analyzed by using the Meta Imaging Series (version 6, Universal Imaging Corporation, West Chester, PA), the LSM 510 imaging software (Carl Zeiss, Inc., Thornwood, NY) and IMARIS (Bitplane AG, Zurich, Switzerland) running on a personal computer.

### 3.4. Results and discussion

Fig. 3 is a two-photon excitation fluorescence image obtained using the GRIN lens probe together with the LSM 510 Meta NLO imaging system showing a renal tubule structure of the rat kidney labeled with Prodan. This image was acquired with the tip of the triplet compound GRIN lens inserted about 3 mm beneath the surface of renal cortex. This depth was determined by the changes of the Z position while the focusing motor of the Zeiss microscope drove the GRIN lens probe into the tissue. The lumen of the tubule is clearly visible. Since the GRIN lens probe is an attachment to the LSM 510 microscope system, we can perform all the different image acquisition modes and using available configurations of the existing microscope system. To demonstrate the capability of using the combination of the GRIN lens probe and the Zeiss

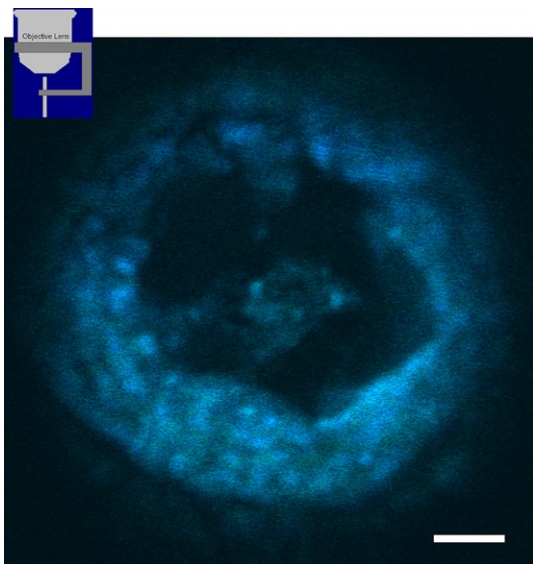


Fig. 3. Fluorescence image of a renal tubule labeled with Prodan acquired using the GRIN lens imaging system. Zoom factor was set to 6. Depth of imaging:  $\sim 3$  mm; excitation: 800 nm; field of view: a  $70 \mu\text{m}$  diameter circle. Scale bar:  $10 \mu\text{m}$ .

LSM 510 system for deep tissue imaging, we acquired Z-stack images of the kidney labeled with Prodan (Fig. 4). The total travel distance of the GRIN lens probe for

acquiring the image stack was  $610 \mu\text{m}$  in the Z direction that started at  $\sim 2.5$  mm beneath the surface of the cortex. Effectively, the range of the imaging depth of this image stack was from  $\sim 2.5$  mm to  $\sim 3.1$  mm in the Z-direction below the kidney surface. This is an adequate depth for imaging the outer medulla (typically 2–4 mm beneath the kidney surface for rat) [27]. It should be noted that the  $610\text{-}\mu\text{m}$  continuous traveling distance of the GRIN lens microendoscopic probe is the limit of the current Zeiss microscope operating system set for automated Z-stack image data acquisition. The travel distance of the Z motor, on the other hand, is on the order of several centimeters that allows further insertion of the GRIN lens probe for deeper tissue imaging. The optical resolution of the GRIN lens imaging system when coupled with a Plan-Apochromat objective ( $20 \times 0.75 \text{ N.A./air}$ ) used for two-photon excitation at 800 nm was about  $0.85 \mu\text{m}$  in the radial direction and axially about  $15 \mu\text{m}$  determined by measurements of  $210 \text{ nm}$  fluorescent beads. Fig. 5 is a montage of images showing a portion of a renal tubule and other detailed kidney structures while the GRIN lens probe was moving deeper into the tissue. These images further demonstrate the capability of the GRIN lens probe for deep tissue microendoscopic imaging. Similarly, in case the GRIN lens probe was used to probe the live kidney tissue stained with cell permeable nuclear dye, as the GRIN lens probe was gradually moving deeper into the tissue, the cells resided in the

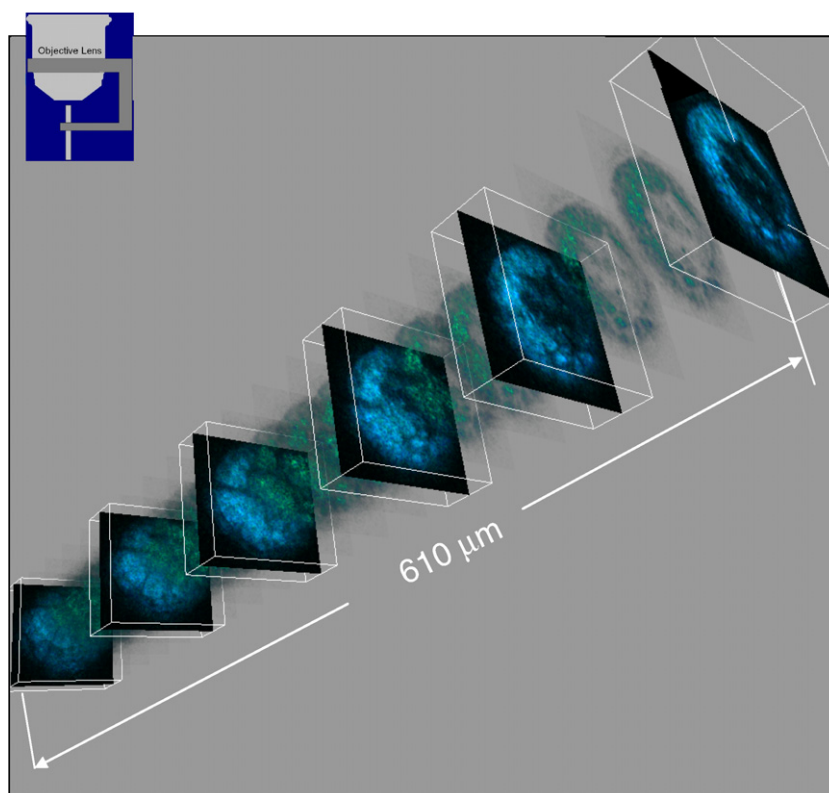


Fig. 4. A Z-series fluorescence image of the kidney stained with Prodan acquired using the GRIN lens imaging system. Z-stack dimension:  $610 \mu\text{m}$ ; depth of imaging: 2.5–3.1 mm beneath the cortex surface; excitation: 800 nm.

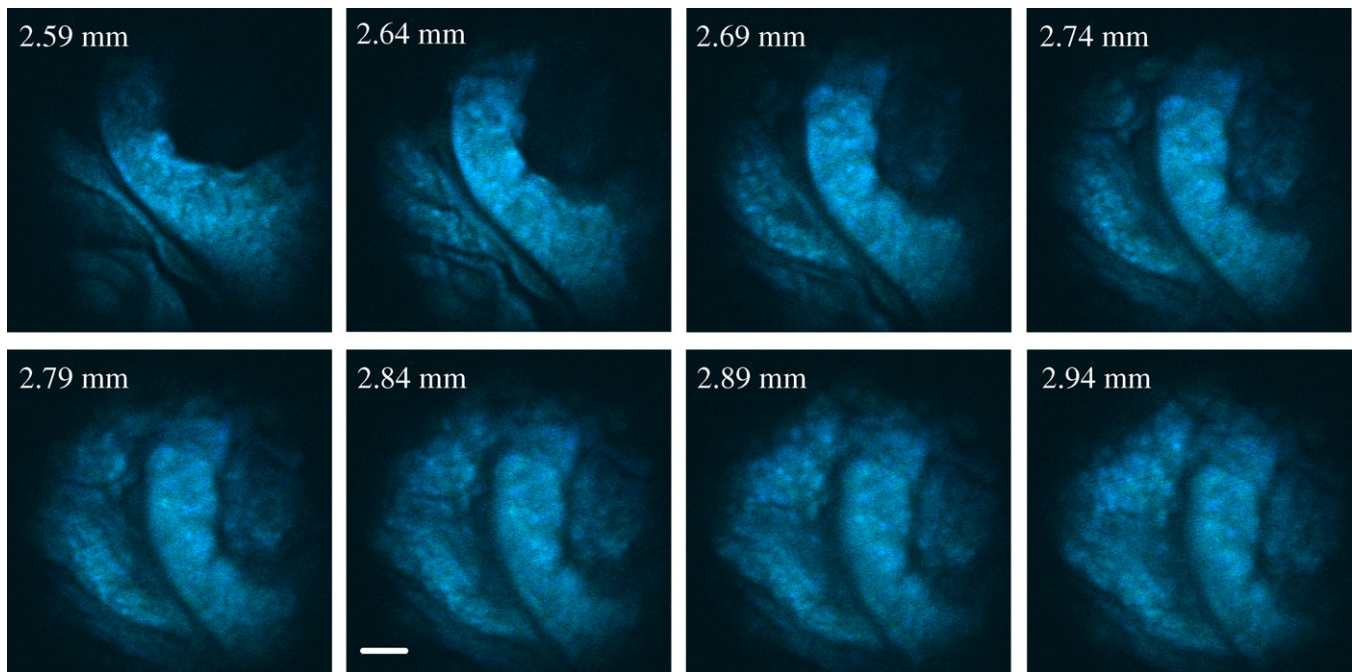


Fig. 5. Montage of images at different depth acquired while the GRIN lens probe was moving deeper into the kidney tissue. A portion of a renal tubule and other structural features was visualized at depth from 2.59 mm to 2.94 mm beneath the kidney surface. Scale bar: 10  $\mu\text{m}$ .

middle of the image (Fig. 6A) moved towards the upper left corner and the cell group which is barely visible and out of focus (cells at the right side of Fig. 6A) moved gradually towards the center of the field of view (Fig. 6D). Thus, cell images at different tissue depth can be recorded and studied. These data suggest that by using this GRIN lens imaging system, it is feasible to achieve deep tissue imaging beyond the 200- $\mu\text{m}$  depth limitations for minimal-invasive kidney investigations without significantly sacrifice the optical resolution.

It is worthwhile to note that the images we obtained by moving of the GRIN lens in the Z-direction are different from 3-dimensional image stacks acquired by using a conventional confocal/two-photon fluorescence microscope. For microendoscopic imaging with the GRIN lens, there was no laser power attenuation at different tissue depths where fluorescence images were acquired. Consequently, the average fluorescent intensities of the images taken at different tissue depth are uniform which can be seen from images of each image series (Figs. 4–6).

One of the reasons we choose to use the triplet configuration which contains two identical imaging lenses used for the objective and coupling lenses is the fact that the GRIN lens probe built in this way has a magnification factor of one. Therefore, it is convenient in acquiring images using the LSM 510 software with correct scaling factors.

There are a number of practical issues of using the GRIN lens probe for in vivo deep tissue imaging we would like to discuss.

First, the field of view of the triplet GRIN lens probe we used is limited to a circle with a diameter ( $D_f$ ) of about 70  $\mu\text{m}$ . The diameter of the circular field of view can be

estimated from the diameter of the GRIN lenses ( $\phi_{\text{lens}}$ ), the pitch lengths of both the relay lens ( $l_{\text{relay-lens}}$ ) and the imaging lenses ( $l_{\text{image-lens}}$ ) as follows,

$$D_f \approx \phi_{\text{lens}} \frac{l_{\text{image-lens}}}{l_{\text{relay-lens}}} \quad (1)$$

The field of view of the GRIN lens probe we used is relatively small. It is inconvenient for imaging larger structures, e.g., a large size tubule or a glomerulus ( $\sim 100 \mu\text{m}$ ). One way to increase the field of view is to use lenses with larger diameters. For example, one could use selected lenses from Grintech GmbH (Frankfurt, Germany) to increase the diameters of the field of view of the triplet GRIN lens probe, e.g., to 94  $\mu\text{m}$  when using 700  $\mu\text{m}$  diameter lenses and to 196  $\mu\text{m}$  with 1000  $\mu\text{m}$  diameter lenses. The adverse effect of using GRIN lenses with increased diameters is the increased possibility of causing tissue trauma when performing microendoscopic measurements. In this regard, it would be beneficial to keep the diameter of the GRIN lens probe small. Alternatively, to increase the field of view with a given GRIN lens diameter, one could either increase the pitch length of the imaging lens or decrease the pitch length of the relay lens. However, it is not possible to increase the pitch length of the imaging lens without decreasing the N.A. of the lens. Theoretically, it is possible to use the imaging lens as a relay lens which could increase the field of view. However, to make it useful, one has to use such a lens with increased numbers of pitches simply to allow the length of the rod (lens) physically long enough to be useful for microendoscopic applications. A concern about using a GRIN lens with increased numbers of pitches is the fact that it could cause

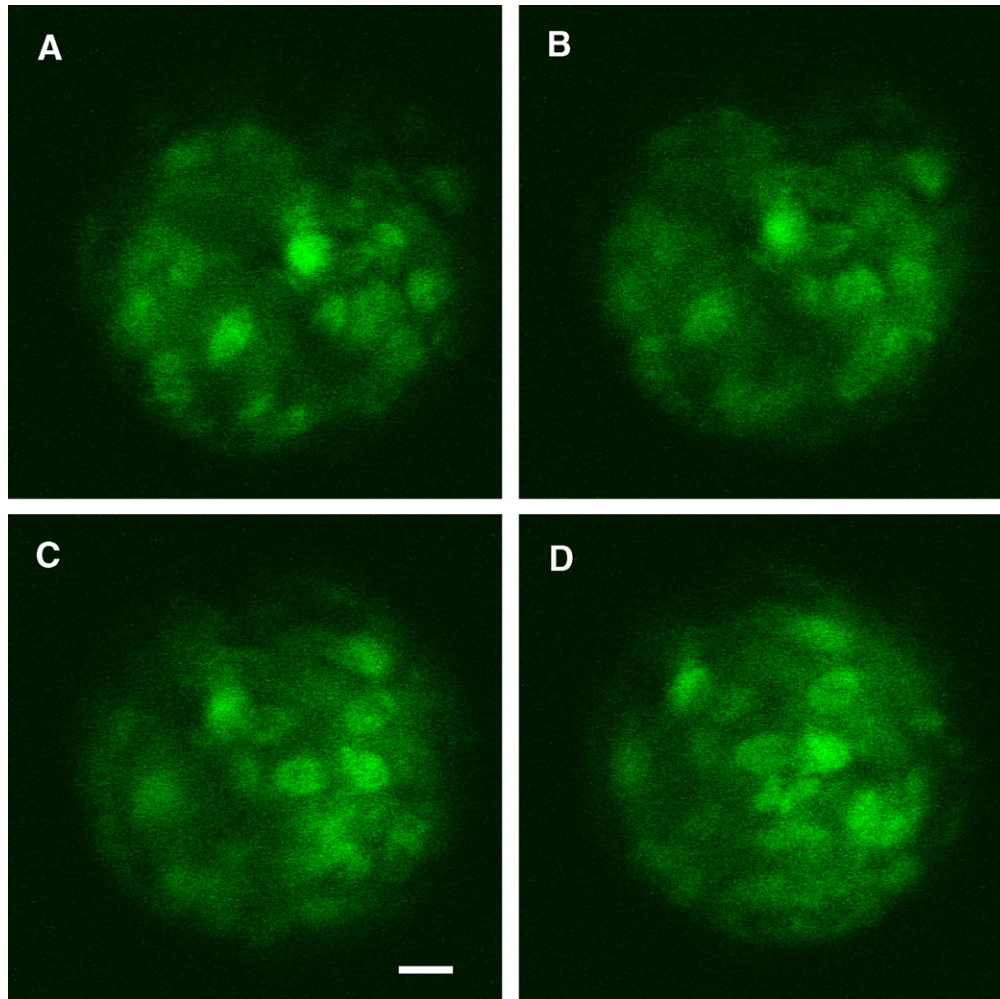


Fig. 6. Microendoscopic images of live kidney stained with nuclear dye. Distance between adjacent images is 50  $\mu\text{m}$ . From A to D the GRIN lens probe moved 150  $\mu\text{m}$  into the kidney tissue and these images recorded the relative movement of the cells passing through the GRIN lens probe. Scale bar: 10  $\mu\text{m}$ .

undesirable nonlinear effects that generate fluorescence within the lens itself when laser light is focused inside the lens [19].

Second, the insertion of the GRIN lens probe into the tissue could cause piercing of local tissues, bleeding and blood clotting. It is difficult to avoid the physical contact between the end surface of the GRIN lens probe with the tissue and blood while performing microendoscopic imaging and, therefore, causing contamination of the imaging lens surface. It is particularly problematic in case when fluorescent dextrans are used to stain the plasma and the dye containing blood contaminates the GRIN lens probe.

In summary, we have demonstrated the feasibility of using a GRIN lens probe for deep kidney tissue microendoscopic imaging. It is advantageous in using the GRIN lens approach to perform deep tissue imaging because of the GRIN lenses are affordable and portable. The GRIN lens probe can also be easily adapted to attach to different commercially available confocal and/or two-photon fluorescence microscope systems. There is a great potential to make the GRIN lens probe an effective tool for in vivo

deep tissue imaging. To that end, it is critically important that one can avoid or minimize local bleeding at the site where the microendoscopic probe should be inserted into the tissue.

#### Acknowledgements

The authors wish to thank Dr. George Rhodes for his expert support in live animal imaging setup, Ashley M. Dutton for her technical support in animal sample preparations and the Indiana Center for Biological Microscopy for using its microscopic imaging facility. The authors also wish to thank Drs. Robert Bacallao, Kenneth Dunn, Pierre Dagher and Timothy Sutton for their supports and stimulating discussions.

This work was supported by a startup funds from an Indiana Genomics Initiative (INGEN) grant from the Eli Lilly and Company Foundation to Indiana University School of Medicine (W. Yu), a pilot study fund from an NIH O'Brien Center of Excellence grant (W. Yu) and an NIH RDK077051 research award on in vivo kidney imaging (W. Yu).

## References

- [1] W. Denk, J.H. Strickler, W.W. Webb, *Science* 248 (1990) 73.
- [2] W. Yu, R.M. Sandoval, B.A. Molitoris, *Am. J. Physiol. Renal. Physiol.* 292 (2007) F1873.
- [3] J.J. Kang, I. Toma, A. Sipos, F. McCulloch, J. Peti-Peterdi, *Am. J. Physiol. Renal. Physiol.* (2006) F495.
- [4] D.R. Larson, W.R. Zipfel, R.M. Williams, S.W. Clark, M.P. Bruchez, F.W. Wise, W.W. Webb, *Science* 300 (2003) 1434.
- [5] P. Theer, M.T. Hasan, W. Denk, *Opt. Lett.* 28 (2003) 1022.
- [6] B. Yu, C.Y. Dong, P.T.C. So, D. Blankschtein, R. Langer, *J. Invest. Dermatol.* 117 (2001) 16.
- [7] C.Y. Dong, B. Yu, P.D. Kaplan, P.T. So, *Microsc. Res. Technol.* 63 (2004) 81.
- [8] K.W. Dunn, R.M. Sandoval, K.J. Kelly, P.C. Dagher, G.A. Tanner, S.J. Atkinson, R.L. Bacallao, B.A. Molitoris, *Am. J. Physiol. Cell Physiol.* 283 (2002) C905.
- [9] W. Yu, R.M. Sandoval, B.A. Molitoris, *Am. J. Physiol. Cell Physiol.* 289 (2005) 1197.
- [10] D.A. Landis, C.J. Seliskar, *Appl. Spectrosc.* 49 (1995) 547.
- [11] M. Vacha, Y. Liu, J. Itho, M. Komuro, T. Tani, H. Nakatsuka, *Rev. Sci. Instrum.* 68 (1997) 254.
- [12] W. Jung, J. Zhang, R. Mina-Araghi, N. Hanna, M. Brenner, J.S. Nelson, Z. Chen, *Lasers Surg. Med.* 35 (2004) 121.
- [13] M. Sato, A. Masuda, H. Ohotaki, N. Tanno, *Opt. Rev.* 10 (2003) 452.
- [14] P.S. Jensen, R. Attariwala, D. Beek, P. Rol, M.R. Glucksberg, *Invest. Ophthalm. Vis. Sci.* 37 (1996) 3876.
- [15] D. Bird, M. Gu, *Opt. Lett.* 28 (2003) 1552.
- [16] J. Knittel, L. Schnieder, G. Buess, B. Messerschmidt, T. Possner, *Opt. Commun.* 188 (2001) 267.
- [17] J.A. Fisher, E.F. Civillico, D. Contreras, A.G. Yodh, *Opt. Lett.* 29 (2004) 71.
- [18] W. Gobel, J.N. Kerr, A. Nimmerjahn, F. Helmchen, *Opt. Lett.* 29 (2004) 2521.
- [19] M.J. Levene, D.A. Dombeck, K.A. Kasischke, R.P. Molloy, W.W. Webb, *J. Neurophysiol.* 91 (2004) 1908.
- [20] J.B. Tan, J. Zhang, *Opt. Laser. Eng.* 42 (2004) 233.
- [21] K. Konig, A. Ehlers, I. Riemann, S. Schenkl, R. Buckle, M. Kaatz, *Microsc. Res. Technol.* 70 (2007) 398.
- [22] J.C. Jung, A.D. Mehta, E. Aksay, R. Stepnoski, M.J. Schnitzer, *J. Neurophysiol.* 92 (2004) 3121.
- [23] F. Helmchen, M.S. Fee, D.W. Tank, W. Denk, *Neuron* 31 (2001) 903.
- [24] S.R. Nova, S. Krol, H.I. de Lasa, *Ind. Eng. Chem. Res.* 43 (2004) 5620.
- [25] L. Fu, X. Gan, M. Gu, *Appl. Opt.* 44 (2005) 7270.
- [26] G.A. Tanner, R.M. Sandoval, B.A. Molitoris, J.R. Bamburg, S.L. Ashworth, *Am. J. Physiol. Renal. Physiol.* 289 (2005) F638.
- [27] B. Flemming, E. Seeliger, T. Wronski, K. Steer, N. Arenz, P.B. Persson, *J. Am. Soc. Nephrol.* 11 (2000) 18.